Journal of Pharmaceutical Sciences 111 (2022) 552–558

Contents lists available at ScienceDirect

Journal of Pharmaceutical Sciences

journal homepage: www.jpharmsci.org

Perspective

Improving Process Understanding in Roll Compaction

Peter Kleinebudde

Institute of Pharmaceutics and Biopharmaceutics, Heinrich Heine University Duesseldorf, Universitaetsstrasse 1, 40225 Duesseldorf, Germany

ARTICLE INFO

Article history:
Received 13 August 2021
Revised 17 September 2021
Accepted 17 September 2021
Available online 22 September 2021

Keywords:
Roll compaction
Process understanding
Scale-up
Process transfer
Process control
Solid fraction
Densification factor

ABSTRACT

Roll compaction/ dry granulation is gaining importance. Numerous papers have been published and many attempts to model the process are available in the meantime. Johanson published a model in 1965, which is the basis for many further modifications until today. The aim of the paper is to improve process understanding in roll compaction, which can be used to setup a roll compaction process, to design a scale-up strategy or to help in process transfer between different types of roll compactors. Based on some assumptions, simple considerations help to estimate a required densification factor and to visualize the relations between roll diameter, gap width and nip angle. Two recently published papers based on simplified Johansen models are used to visualize the relations between specific compaction force and the maximal pressure experienced by the material. The influence of roll diameter, gap width and compressibility constant are discussed. This helps to estimate, if a scale-up or process transfer is reasonable. The recently introduced dimensionless Midoux-number can also be used to design scale-up or process transfer of roll compaction without knowledge about the maximal pressure. Exploring the simple concepts can help to improve process understanding even without a background in engineering.

Introduction

Compared with wet granulation, roll compaction/ dry granulation (RCDG) is less complicated saving time and costs.[1] Due to improvements in machine design and process control in the past decades, RCDG is nowadays no longer only used for water or heat sensitive APIs, but has become a standard technique in pharmaceutical manufacturing.[2]

In RC, a starting material is fed to a zone with two counterrotating rolls (Fig. 1). The starting density is between its untapped bulk density and tapped bulk density. There is a density gradient towards the closest distance between the two rolls, the gap width (S). When the material is in contact with the rolls, several regions can be distinguished: in the slip zone the speed of the rolls is higher than the speed of the material. Due to increasing friction between the material and the rolls, which is related to increasing density, the material starts at a certain point to move with the same speed as the roll speed in the nip zone. The nip angle (α) separates the slip zone and the nip zone. A pre-densification takes place in the slip zone, but the main densification happens in the nip zone. Many models assume that velocity of the material in the nip zone is uniform span-wise, i.e. the mass flow between the rolls is constant along the axis perpendicular to the rolls.[3,4] With this assumption, a densification factor (DF) can be defined as the ratio of N/S (Fig. 1), where N is the nip width. The produced ribbon increases in thickness due to elastic recovery in the exit zone after passing the gap.[5] Thus, the ribbon thickness (T) exceeds the gap width in many cases.

The assumption of a uniform velocity is not strictly correct.[6,7] The velocity of the material transport is not uniform span-wise between the two rolls in the nip zone. However, in a controlled state during production, the non-homogeneous flow does not limit the following considerations and is ignored. Furthermore, the elastic recovery is ignored, which is of importance in predicting ribbon densities.[5] Since a constant elastic recovery for a material can be expected at constant stress, this factor can be ignored for scale-up or process transfer.

The following considerations use the roll width just for calculating the specific compaction force (SCF in kN/cm), which is the compaction force divided by the roll width. Other effects of the roll width are not considered.[8] The roll speed, which can affect P_{max}[9,10] or elastic recovery, is ignored in the context of this paper. Another simplification is the use of a mean solid fraction (SF) or porosity (ε) of ribbons.

Symbols and abbreviations: α, nip angle; Δ, difference in gap width; ε, porosity; θ, angle; ρ, density; σ, stress; API, active pharmaceutical ingredient; D, roll diameter; DF, densification factor; f, correction factor; K, compressibility constant; Mi, Midoux number; N, N', nip width (distance between the rolls at nip angle); P, pressure; P_{max}, maximum pressure experienced by the material in roll compaction; RCDG, roll compaction/ dry granulation; RS, roll speed; S, gap width (distance between the two rolls at 0°); SCF, specific compaction force; SF, solid fraction; t, time; T, ribbon thickness; W, roll width.

E-mail address: kleinebudde@hhu.de

https://doi.org/10.1016/j.xphs.2021.09.024

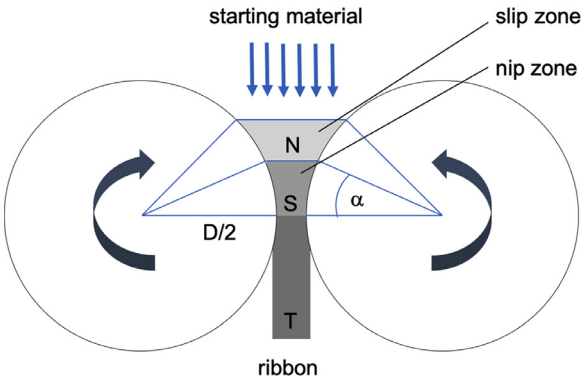

Figure 1. scheme of roll compaction with D: roll diameter, N: nip width, S: gap width, T: ribbon thickness, α: nip angle.

In reality, ribbons have a spatial distribution of SF or ε.[11,12] Again, the simplification is not relevant for the basic considerations in this paper. The type and quality of the sealing system is not taken into account. Several of the neglected factors are discussed in more detail by Michrafy et al.[13]

$$SF = \frac{\rho_{bulk/particle}}{\rho_{true}} = 1 - \varepsilon \qquad \text{(eq. 1)}$$

SF is the ratio of a bulk density or particle density to the true density of the material Equation (1). If the porosity is zero, SF is 1. SF_{gap} is the ratio of the density of the material in the gap to the true density, SF_{ribbon} the ratio of ribbon density after elastic recovery to the true density of the material. The SF_{ribbon} is an intermediate CQA of ribbons, since it affects the granule size distribution, granule SF, flowability and tabletability among others. Thus, a common goal in RCDG is to keep the SF_{ribbon} constant over time.[14] Achieving a constant SF_{ribbon} is also an issue in scale-up or in process transfer to another type of roll compactor. Due to elastic recovery, $SF_{ribbon} \leq SF_{gap}$. In the following, SF_{gap} is considered.

Roll compactors on the market can be divided in systems with fixed gap width, where both rolls have a fixed position, and variable gap width, where only one roll is fixed (master roll) and the second one is movable (slave roll). The SCF in fixed gap systems is a result of the screw speed of the feeding and/or tamping screw and the roll speed. Fluctuations in the feed rate at constant roll speed will automatically result in fluctuations in SCF and consequently in SF_{gap}. The feeding system is crucial in achieving a constant feed rate. One main aim of granulation is the improvement of flowability. Therefore, the starting materials often have poor flowability, which makes constant dosing difficult. Changes in SCF, which result from fluctuations in feed rate in fixed gap systems, are crucial for SF_{gap}.

When using a variable gap system, SCF can be held constant in case of variable feed rates by a fast controller: in case of overfeeding, the gap opens and vice versa. The varying gap width is also influencing SF_{gap}, but to a much smaller extent than variable SCF. Thus, the variable gap systems possess a huge advantage. Modern roll compactors go even a step further. By introducing a second controller, which is slower than the controller of the SCF, it is possible to keep both, SCF and gap width, constant. The second controller adapts the feeding and/ or tamping screw speed in order to keep the gap width constant. This is called “gap control”, which is implemented in several modern roll compactors. Depending on the type of control system, the independent and dependent variables differ: In a fixed gap system, the screw speed and roll speed are independent and the SCF is variable. In a force controlled variable gap system, the screw speed and the SCF are independent, the roll speed is fixed and the gap width is variable. In a gap-controlled system, SCF and gap width are independent, the roll speed is fixed and the screw speed is variable. This distinction is important when comparing articles about roll compaction, because the conclusion depend on the type of the used system.

Some equipment providers offer roll compactors with different roll diameters and roll widths. Others have only machines with the same roll diameter, but different roll width. Since a change in roll diameter is relevant for the selection of process parameters (see below), a scale-up is easier for machines with the same roll diameter, but different roll width.

There are several approaches for scale-up or process transfer available, either based on mechanistic models,[8,15-21] statistical approaches[22] or hybrid modeling.[23] The aim of the paper is to describe some basic relations between important variables in RC including machine variables like D, process variables like SCF and S, material variables and resulting variables like SF_{ribbon}, nip angle or DF. After starting with some geometric considerations two recently published simplified models[24,25] are used to visualize the relations. This is a brief supplement to the studies already published.

Estimation of DF

It is useful to have an idea about the required DF in order to design a roll compaction process. DF can be estimated by using SF of the starting material and the ribbon. The use of SF allows a material independent comparison of the changes during densification. A first suggestion is to express the untapped or tapped bulk density of the starting material as SF_{bulk}, because the density at the point of entry to the nip zone is expected to be in this range. A common recommendation is that SF_{ribbon} is in the range of 0.6-0.8.[26] If the target SF_{ribbon} and the range of SF_{bulk} are known, a range for the required DF can be estimated Equation (2):

$$DF = \frac{SF_{ribbon}}{SF_{bulk}} \approx \frac{SF_{gap}}{SF_{bulk}} \qquad \text{(eq. 2)}$$

Bulk, tapped and true densities can be measured easily or taken from suppliers of materials in order to calculate SF_{bulk}. SF_{bulk} for microcrystalline cellulose is in a range of 0.15–0.3. If the target SF_{ribbon} is 0.6 in this case, DF is in the range of 2–4. Untapped SF_{bulk} for a lactose may be 0.43 and tapped SF_{bulk} 0.6. If the target SF_{ribbon} is 0.8, the range for DF is 1.3 to 1.9. The untapped bulk SF of a calcium phosphate may be 0.27. A DF of 3 is required to achieve a SF_{ribbon} of 0.8.

If the target SF_{ribbon} is in the range of 0.6–0.8 and the DF is 5, the SF_{bulk} of the starting material is in the range of 0.12–0.16, which is quite low. Thus, a DF higher than 5 or 6 is usually not expected. On the other hand, if the SF_{bulk} of the starting material is already 0.5, the maximal achievable DF is 2.

In a RC process, SF_{gap} can be estimated from the material density at gap (ρ_{gap}). For this purpose, the mass of ribbons can be determined by collecting the ribbons on a balance, e.g. for a minute. In steady state the mass flow should be constant. The volume, which is passing the gap, e.g. during one minute, can be calculated by Equation (3).[3]

$$V = S \cdot W \cdot \pi \cdot \left(D + \frac{S}{2}\right) \cdot RS \cdot t \qquad \text{(eq. 3)}$$

with W=roll width, RS=roll speed in RPM and t=time in min.

The use of (estimated) SFs of the starting material and the ribbon allows easily an estimation of the required DF.

Densification Factor and Nip Angle

Taking the assumptions mentioned in the Introduction into account, the densification factor and the nip angle (Fig. 1) are related. $\cos(\alpha)$ can be derived from geometric considerations Equation (4).[23] This allows the calculation of N Equation (5), which is used for calculating DF Equation (6).[3] At the same time DF is the ratio of SF in the gap and SF at nip angle.

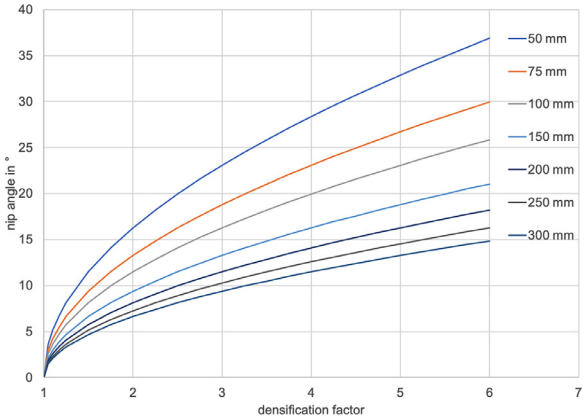

Figure 2. relation between DF and nip angle depending on roll diameter for a gap width of 2 mm.

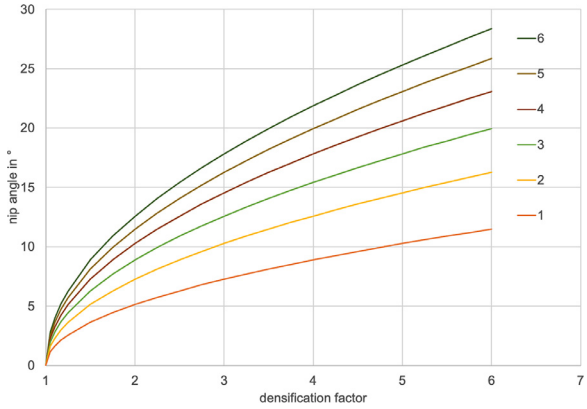

Figure 4. relation between DF and nip angle depending on gap width; a) roll diameter 100 mm, b) roll diameter 250 mm.

$$\cos\alpha = \frac{D+S-N}{D} \quad \text{(eq. 4)}$$

$$N = D+S-D\cdot\cos\alpha \quad \text{(eq. 5)}$$

$$DF = \frac{N}{S} = \frac{D+S-D\cdot\cos\alpha}{S} = \frac{SF_S}{SF_\alpha} \quad \text{(eq. 6)}$$

The nip angle is influenced by the roll diameter, the gap width and the densification factor. A higher *DF* is related to a higher nip angle at constant gap width and roll diameter (Figs. 1, 2, 4). Assuming a constant density at the nip angle, more material has to be compressed to reach a higher DF at constant gap width, thus N and α must be higher.

Figure 2 shows the relation between DF and nip angle depending on the roll diameter. If the required DF is known, the nip angle can be calculated for a given roll diameter at a specific gap width. Roll diameters of 50 mm to 300 mm are common for pharmaceutical purposes. The larger the roll diameter is, the smaller is the nip angle for a given DF and gap width. The influence of roll diameter is especially high for rolls with diameters ≤ 100 mm. At a gap width of 2 mm, the range of nip angles for DF from 2 to 4 is 7° to 28°. High nip angles are more difficult to achieve, which explains why RC is often easier to perform on roll compactors with larger roll diameters.

The nip width for a small roll diameter (N') is lower than the nip width for a larger roll diameter (N) for a given nip angle (Fig. 3). Thus, N'/S < N/S, since S is constant. DF is lower for a small roll diameter at constant gap width and nip angle. In contrast, the nip angle for a small roll diameter has to be higher in order to keep DF constant at constant gap width (Fig. 2).

Figure 4 shows the relation between DF and nip angle depending on the gap width. If the required DF is known, the nip angle can be calculated for a given gap width at a specific roll diameter. Gap widths of 0.5 mm to 6 mm are possible and 2 mm to 4 mm are common for pharmaceutical purposes. The larger the gap width is, the higher is the nip angle for a given DF and roll diameter. The influence of a change in gap width is especially high for small gaps. The range of nip angles for DF from 2 to 4 is 5° to 22° for 250 mm roll diameter.

Since N/S > (N+Δ)/(S+ Δ), a higher gap width results in a lower DF at constant roll diameter and nip angle (Fig. 5). E.g. if N is 3 and S is 2 and Δ is 1, 3/2 = 1.5 > 1.33 = (3+1)/(2+1) = 4/3. The nip angle must increase when opening the gap to keep DF constant.

Since high nip angles are more difficult to achieve at the beginning of a RC process for some materials, it can be recommended in these cases to use a small gap width in the beginning and then open the gap during the process. Due to the low nip angle at low gap width in the beginning, the process can start and a ribbon is produced. By opening the gap during the process, the process is not interrupted and the nip angle will increase.

So far, the calculations are material independent and just based on geometric considerations. They allow a rough estimation of the required process. They are relevant, if the process is transferred between roll compactors of different diameters or if the gap width is opened in order to achieve a higher throughput. The nip angle will change, if the target DF has to be kept constant.

Applying the Simplified Johanson Model After So et al. (24)

General Considerations

In the context of improving process understanding, some qualitative relationships should be elucidated. The focus is not on absolute

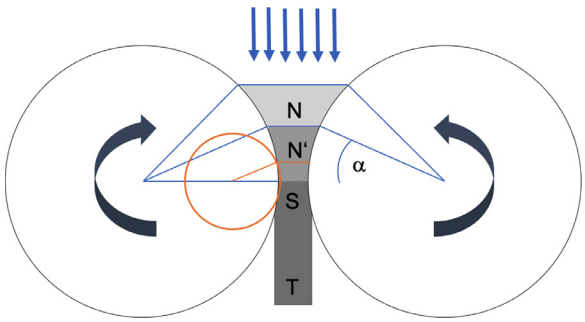

Figure 3. reducing the roll diameter at constant nip angle and constant gap width results in a decrease of DF.

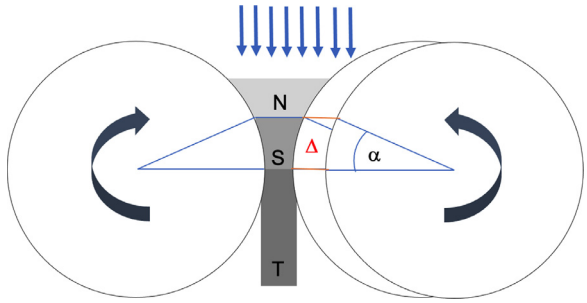

Figure 5. increasing gap width at constant nip angle and constant roll diameter results in a decrease of DF.

values, but on illustrating relations between equipment variables like roll diameter, process variables like SCF, gap width and material variables like compressibility constant (K). K is the slope in a lnρ-lnP diagram in uniaxial compression. A rough estimation of reasonable values helps to improve process understanding. This can be used in the context of scale-up and process transfer between different roll compactors. Therefore, simplified models are used to make the required calculations easy for everybody.

Johanson[27] published a model for the roll compaction of granular materials. The granular material was considered compressible and cohesive in a continuous model. The granular material is described by the internal friction angle, the wall friction angle and the compressibility constant (K). Many authors developed the model further and made modifications.[4,9,18,21,28-30] The original model and the modifications have merits.

Recently, So et al.[24] proposed a simplified Johanson's model, which can assist process understanding without using complicated methods. The relation between SCF and the maximum pressure experienced by the material in roll compaction (P_{max}), is analyzed. Furthermore, the SCF-SF relationship can be obtained. The authors discovered that above a certain wall friction angle, the SCF-P_{max} relationship becomes insensitive to both friction angles. The compressibility constant is the only material property left (e.g. MCC: 3.1, mannitol 7.3, dicalcium phosphate anhydrate: 13.0). The simplified model allows to calculate the SCF-P_{max} and the SCF-SF relationship for any given roll geometry, if the compressibility constant of the material is known.

To compensate a span-wise velocity gradient, the authors implemented a mass correction factor (f), which was fixed to 1.03 according to the performed measurements. Following Bi et al.[29], the correction factor was presented outside the integral.

$$P_\theta = P_{max} \cdot \left[\frac{\frac{S}{D}}{\left(1 + \frac{S}{D} - \cos\theta\right)\cos\theta} \right]^K \cos\theta \qquad \text{(eq. 7)}$$

$$SCF = \frac{P_{max} \cdot D}{2} \cdot f^K \cdot \int_{\theta=0}^{\theta=20^\circ} \left[\frac{\frac{S}{D}}{\left(1 + \frac{S}{D} - \cos\theta\right)\cos\theta} \right]^K \cos\theta d\,\theta \qquad \text{(eq. 8)}$$

with f = correction factor (f = 1.03), K = compressibility constant, S = gap width and D = roll diameter.

The correction factor of 1.03 was used for the shown figures. This correction factor is based on limited results and may be corrected in the future. A correction will change the absolute values, but the trends and relations are not affected.

Assuming a certain P_{max}, a pressure-angle curve can be calculated according to Equation (7) for constant values of D, S and K. SCF can be calculated according Equation (8), which requires the integration of the pressure angle curve. So et al.[24] recommend an integration for angles in the range of 0° to 20°. Since SCF is used as a parameter in the RC process, P_{max} is not immediately known. Some roll compactors show a pressure instead of SCF, but this is a hydraulic pressure and should not be confused with P_{max}.

The (critical) nip angle was defined by So et al.[24] as the angle, where 95% of the area under the pressure-angle curve is achieved (Fig. 6). In the following, a different proposal is used: The nip angle is the angle, where the pressure drops below 2 MPa. This helps to identify the influence of P_{max} and SCF on nip angle. The original proposal of 95% of the area is less sensitive to these effects. The nip angle in Figure 6 is 9.0° according to the new definition.

Lower wall friction angles lead to lower nip angles. This is the reason for higher P_{max} values for a specific SCF. P_{max} has to be higher at low nip angle to keep SCF ($\sim$ area under the pressure-angle curve) constant. The most efficient way to increase the nip angle is to increase the wall friction. The use of rolls with a textured surface instead of a polished, smooth roll is a common way to increase the wall friction angle. So et al.[24] claim that a critical wall friction angle of 22° is exceeded when using knurled rolls, which enables the application of the simplified model.

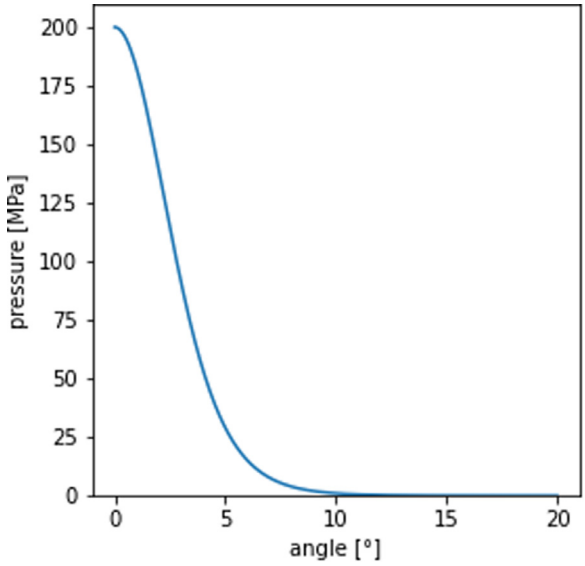

Figure 6. pressure-angle relationship (D=250 mm, S=2 mm, K=5).

For a detailed description of the simplified model the reader is referred to So et al.[24] Some relations can be visualized by applying this simplified model.

Relation Pressure-Angle

Figure 7: a) influence of roll diameter on the pressure-angle relation at constant P_{max}, S and K; b) influence of gap width on the pressure-angle relation at constant P_{max}, D and K; c) influence of compressibility constant on the pressure-angle relation at constant P_{max}, D and S

The curves in Figure 7 always have the same P_{max}, but vary in roll diameter (Fig. 7a), gap width (Fig. 7b) or compressibility constant (Fig. 7c). The pressure drop is steeper for small gaps, large roll diameters and higher compressibility constants. A steeper pressure drop is associated with a lower nip angle. Achieving the same pressure requires a lower gap width or a higher roll diameter. Materials with a higher compressibility constant show lower nip angle. Since materials with a low compressibility constant like microcrystalline cellulose show a high nip angle, the process start can be more complicated in these cases. As recommended earlier, starting with a smaller gap – associated with a smaller nip angle – can help to produce a ribbon; then the gap can be opened during the process to the target value.

Relation SCF-P$_{max}$

The applied SCF translates to a P_{max} in a certain roll compaction process. This relation is dependent on different variables. Gap width, roll diameter and compressibility constant all have a high influence on the relation between SCF and P_{max}. With increasing roll diameter (Fig. 8a), increasing gap width (Fig. 8b) and a lower compressibility constant (Fig. 8c), a higher SCF is required to achieve the same P_{max}. At a constant SCF, P_{max} increases with decreasing gap width, decreasing roll diameter and increasing compressibility constant.

Most roll compactors have a limit for SCFs of maximal 20 kN/cm. Figure 8 allows a rough estimation, which P_{max} can realistically achieved for some combinations of D, S and K. Other combinations can be calculated using Equations (7) and (8).

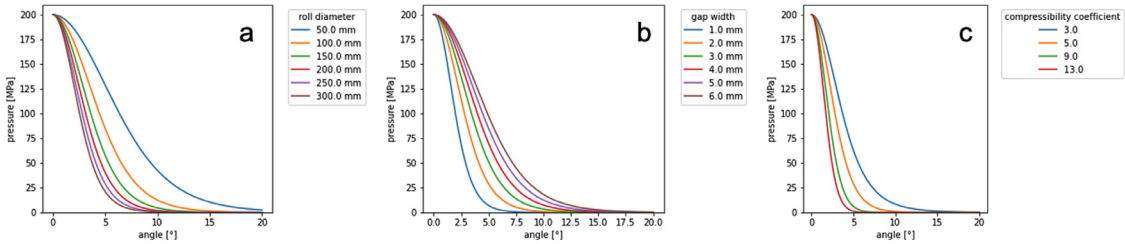

Figure 7. a) influence of gap width on the pressure-angle relation at constant P_{max}, D and K; b) influence of roll diameter on the pressure-angle relation at constant P_{max}, S and K; c) influence of compressibility constant on the pressure-angle relation at constant P_{max}, D and S.

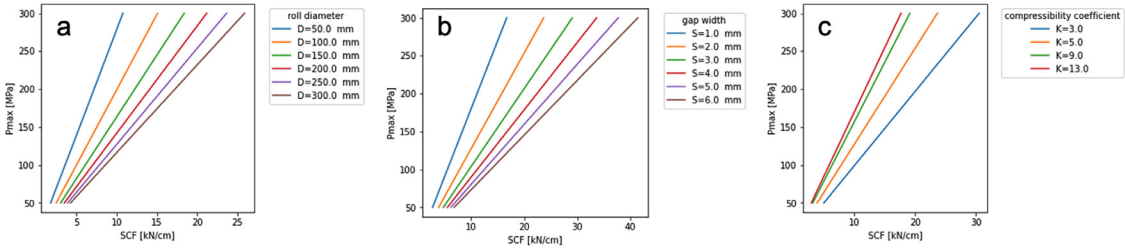

Figure 8. a) influence of roll diameter on the relation between SCF and P_{max} (S=2 mm, K=5), b) influence of gap width on the relation between SCF and P_{max} (D=250 mm, K=5), c) influence of compressibility constant on the relation between SCF and P_{max} (D=250 mm, S=2 mm).

Relation P_{max}*-DF and SCF-DF*

Figure 9 illustrates the relation between SCF or P_{max} and DF. DF raises with increasing SCF or P_{max} at constant values for D, S and K.

Changing the roll diameter has a marginal influence on DF at constant P_{max} (Fig. 9a), but a high influence at constant SCF (Fig. 9b). At constant SCF, DF is lower for large roll diameter. For roll diameters between 100 mm and 300 mm the effect of roll diameter on the P_{max}-DF relationship is negligible; the effect is relevant only for lower roll diameters. A desired DF can be achieved within narrow limits, if P_{max} is held constant, but not at constant SCF. Therefore, it is recommended to keep P_{max} constant[15,18,20] in scale-up or process transfer. However, P_{max} cannot be chosen directly in the process.

Similar observations can be made for a change in gap width. The influence on the P_{max}-DF relationship (Fig. 9c) is much less than for the SCF-DF relationship (Fig. 9d). A constant SCF results in lower DF at larger gap width. Again, for scale-up by increasing the gap width, P_{max} should be kept constant rather than SCF.

Materials or formulations with different compressibility constants influence both relations of P_{max}-DF and SCF-DF (Fig. 9e,f). For each formulation a suitable setting has to be established. Knowing the compressibility constant, values of SCF or P_{max} can be estimated based on experience with other materials. A certain P_{max} or SCF results in a higher DF for materials with lower compressibility constant.

Relation P_{max}*-Nip Angle and SCF-Nip Angle*

A higher P_{max} or SCF leads to a higher nip angle (Fig. 10). Since the DF raises with P_{max} or SCF and since DF and nip angle are related (Fig. 4), the nip angle is higher for large values of P_{max} and SCF. Decreasing the roll diameter, increasing the gap width or decreasing the compressibility constant lead to larger nip angles at a certain P_{max} or SCF. This was illustrated in Figure 7 for a P_{max} of 200 MPa. Similar relations are seen for other values of P_{max}. Changes in roll diameter or gap width are related with different nip angles. Because

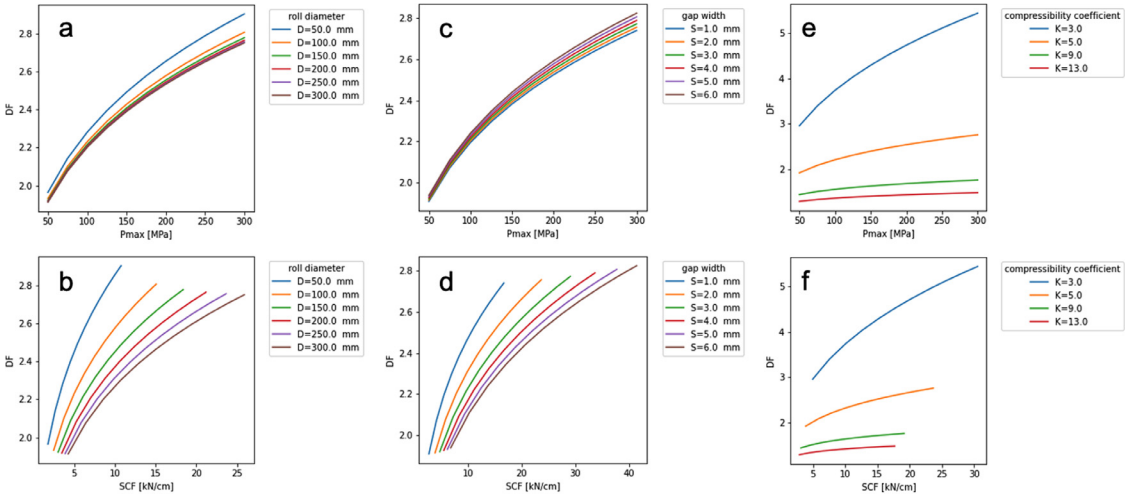

Figure 9. influence of roll diameter on the relation between a) P_{max} and DF, b) SCF and DF, influence of gap width on the relation between c) P_{max} and DF, d) SCF and DF, influence of compressibility constant on the relation between e) P_{max} and DF, e) SCF and DF

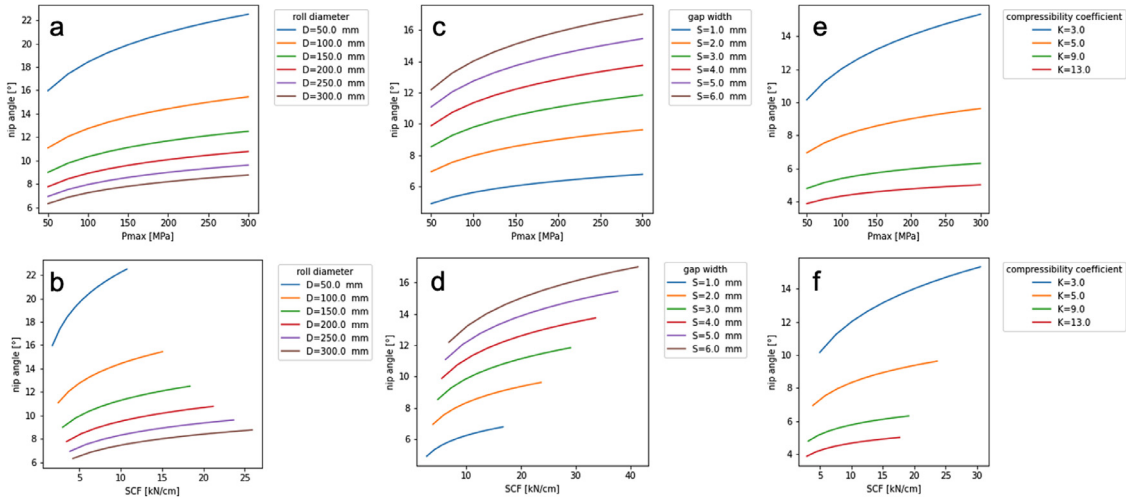

Figure 10. influence of roll diameter on the relation between a) P_{max} and nip angle, b) SCF and nip angle (S=2 mm, K=5), influence of gap width on the relation between c) P_{max} and nip angle, d) SCF and nip angle (D=250 mm, K=5), influence of compressibility constant on the relation between e) P_{max} and nip angle, f) SCF and nip angle (D=250 mm, S=2).

the feed of the material between the rolls is more difficult at high nip angles, the gap can be closed to start a process and then opened to run the process at the desired gap width.

In summary, the simplified model of So et al.[24] helps to understand relations in RC processes and helps to design these processes. The authors have performed an experimental verification of the model by using three excipients with values for K between 3 and 13. An overprediction of P_{max} was compensated by introducing a correction factor Equation (8). The authors proposed to build a "Virtual Roll Compactor". By entering the known variables D, S and K, the resulting values for P_{max} and SF_{ribbon} are calculated. This facilitates the setup of a RC process or the transfer to a different roll compactor.

Applying the Midoux number

Sousa et al.[25] proposed a dimensionless number, called Midoux number (Mi), to assist process transfer and scale-up. The starting point is again the model of Johanson.[27] The authors derive a model, which does not require the internal friction angle and the wall friction angle. This is in line with the thin-layer model derived from uniaxial compression.[3] Further simplifications were made, which lead to errors below 5% for K > 3.5 and DF > 2. These limits are valid for many materials and RC processes. Finally, the authors estimate the stress in the gap (σ_S) by Equation (10). The stress at the nip angle is unknown, and is assumed to be 2 MPa in the following calculations.

$$\frac{\sigma_S}{\sigma_\alpha} = \left(\frac{\rho_S}{\rho_\alpha}\right)^K = DF^K \qquad \text{(eq. 9)}$$

$$\sigma_S \approx \frac{2SCF}{D}\sqrt{\frac{2K}{\pi S/D}} \qquad \text{(eq. 10)}$$

The authors applied Equation (10) in Equation (9) to yield the dimensionless Midoux number Equation (11). Mi can be used for a first approximation how P_{max} is influenced by SCF, D, S and K.

$$Mi = \frac{2SCF}{D\sigma_\alpha}\sqrt{\frac{2K}{\pi S/D}} = DF^K \qquad \text{(eq. 11)}$$

Mi can be used for process transfer and scale-up. Keeping Mi constant, when changing roll diameter and/or gap width results in the same densification factor. For a specific material, K can be neglected and the process parameters should be adjusted in a way that Mi is constant. This is achieved by keeping $SCF\sqrt{\frac{1}{SD}}$ constant. This can be used to keep SF_{gap} constant when changing the equipment. For a detailed description of the simplified model the reader is referred to Sousa et al.[25]

When using the concept of keeping $SCF\sqrt{\frac{1}{SD}}$ constant for a given material, it can be recommended to keep the product of roll diameter and gap width constant in order to get the same SCF and P_{max} when changing the roll diameter. Figure 11a illustrates this for "Midoux pairs" with constant product of D and S. Changing the roll diameter from 100 mm to 300 mm by adapting the gap width leads to constant relation between SCF and P_{max}. If the gap width is not adjusted, SCF varies for a given P_{max} by changing the roll diameter (Fig. 8a). The DF varies in a small range for a constant P_{max} (Fig. 11b). This is similar to a change in diameter without adapting the gap width (Fig. 9d). The

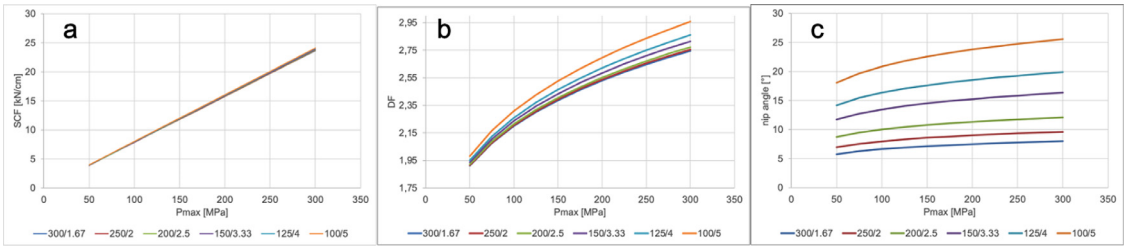

Figure 11. Results for "Midoux pairs" of D [mm]/S [mm] (legend) with constant product $D \cdot S$: a) relation between SCF and P_{max}, b) relation between SCF and DF, c) relation between SCF and nip angle.

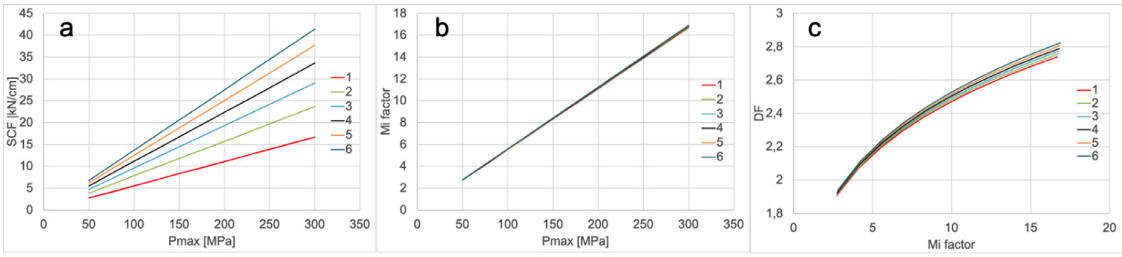

Figure 12. a) relation between SCF and P_{max} for D=250 mm, K=5 and S=1-6 mm (legend), b) relation between P_{max} and Mi factor ($SCF \cdot \sqrt{1}/S$), c) relation between Mi factor and DF.

approach helps to design a scale-up regarding the roll diameter. The nip angle is not constant for the "Midoux pairs" (Fig. 11c), which can be expected due to the dependency on D and S.

If the gap is changed for a given roll compactor (= constant D), SCF will vary for a constant P_{max} (Fig. 12a). In order to calculate the appropriate SCF for a change in gap width, the simplified Mi factor ($SCF \cdot \sqrt{1}/S$) can be calculated. The relation between the Mi factor and P_{max} is unique (Fig. 12b) and DF shows only minor variations for a nearly constant Mi factor (Fig. 12c). Thus, an adjustment of SCF for a change in gap width can be calculated by the Mi factor.

A simultaneous change in roll diameter and gap width can also be handled by this concept. This provides an easy approach for a starting point of validating experiments.

Sousa et al.[25] have shown results for different formulations and ranges for D from 120 mm to 250 mm, for S from 2 mm to 4 mm and for SCF from 2.1 kN/cm to 16 kN/cm. A good correlation between the Mi number and DF was found across all settings. DF varied in the range of 1.8 to 3.2. This approach is helpful in designing a process and for scale-up and process transfer.

Funding Sources

This research did not receive any specific grant from funding agencies in the public, commercial, or not-for-profit sectors.

Declarations of Competing Interest

None

Acknowledgments

Lenny Paola Espinoza Luna wrote a Python script, which visualize the results of the simplified Johanson model (Figs. 6-10). The author thanks Hannah Lou Keizer, Klaus Knop, Rok Sibanc and Raphael Wiedey for constructive feedback on an earlier version of the manuscript.

References

1. Leane M, Pitt K, Reynolds G. The manufacturing classification system working G. A proposal for a drug product Manufacturing Classification System (MCS) for oral solid dosage forms. *Pharm Dev Technol*. 2015;20:12–21.
2. Kleinebudde P. Roll compaction/dry granulation: pharmaceutical applications. *Eur J Pharm Biopharm*. 2004;58(2):317–326.
3. Peter S, Lammens RF, Steffens K-J. Roller compaction/Dry granulation: use of the thin layer model for predicting densities and forces during roller compaction. *Powder Technol*. 2010;199(2):165–175.
4. Muliadi AR, Litster JD, Wassgren CR. Modeling the powder roll compaction process: comparison of 2-D finite element method and the rolling theory for granular solids (Johanson's model). *Powder Technol*. 2012;221:90–100.
5. Keizer HL, Kleinebudde P. Elastic recovery in roll compaction simulation. *Int J Pharm*. 2020;573:118810.
6. Michrafy A, Ringenbacher D, Tchoreloff P. Modelling the compaction behaviour of powders: application to pharmaceutical powders. *Powder Technol*. 2002;127(3):257–266.
7. Mazor A, Perez-Gandarillas L, de Ryck A, Michrafy A. Effect of roll compactor sealing system designs: a finite element analysis. *Powder Technol*. 2016;289:21–30.
8. Alleso M, Holm R, Holm P. Roller compaction scale-up using roll width as scale factor and laser-based determined ribbon porosity as critical material attribute. *Eur J Pharm Sci*. 2016;87:69–78.
9. Bindhumadhavan G, Seville JPK, Adams MJ, Greenwood RW, Fitzpatrick S. Roll compaction of a pharmaceutical excipient: experimental validation of rolling theory for granular solids. *Chem Eng Sci*. 2005;60(14):3891–3897.
10. Patel BA, Adams MJ, Turnbull N, Bentham AC, Wu CY. Predicting the pressure distribution during roll compaction from uniaxial compaction measurements. *Chem Eng J*. 2010;164(2-3):410–417.
11. Wiedey R, Kleinebudde P. Infrared thermography - a new approach for in-line density measurement of ribbons produced from roll compaction. *Powder Technol*. 2018;337:17–24.
12. Miguelez-Moran AM, Wu CY, Dong H, Seville JP. Characterisation of density distributions in roller-compacted ribbons using micro-indentation and X-ray microcomputed tomography. *Eur J Pharm Biopharm*. 2009;72(1):173–182.
13. Michrafy A, Zavaliangos A, Cunningham JC. 4 - Dry granulation process modeling. In: Pandey P, Bharadwaj R, eds. *Predictive Modeling of Pharmaceutical Unit Operations*. Cambridge: Woodhead Publishing; 2017:71–97.
14. Sun CC, Kleinebudde P. Mini review: mechanisms to the loss of tabletability by dry granulation. *Eur J Pharm Biopharm*. 2016;106:9–14.
15. Souihi N, Reynolds G, Tajarobi P, et al. Roll compaction process modeling: transfer between equipment and impact of process parameters. *Int J Pharm*. 2015;484(1-2):192–206.
16. Boersen N, Belair D, Peck GE, Pinal R. A dimensionless variable for the scale up and transfer of a roller compaction formulation. *Drug Dev Ind Pharm*. 2016;42:60–69.
17. Nesarikar VV, Patel C, Early W, Vatsaraj N, Sprockel O, Jerzweski R. Roller compaction process development and scale up using Johanson model calibrated with instrumented roll data. *Int J Pharm*. 2012;436(1-2):486–507.
18. Reynolds G, Ingale R, Roberts R, Kothari S, Gururajan B. Practical application of roller compaction process modeling. *Comp Chem Eng*. 2010;34(7):1049–1057.
19. Rowe JM, Crison JR, Carragher TJ, Vatsaraj N, McCann RJ, Nikfar F. Mechanistic insights into the scale-up of the roller compaction process: a practical and dimensionless approach. *J Pharm Sci*. 2013;102(10):3586–3595.
20. Toson P, Lopes DG, Paus R, et al. Model-based approach to the design of pharmaceutical roller-compaction processes. *Int J Pharm-X*. 2019;1:100005.
21. Amini H, Akseli I. A first principle model for simulating the ribbon solid fraction during pharmaceutical roller compaction process. *Powder Technol*. 2020;368:32–44.
22. Liu Z, Bruwer M-J, MacGregor JF, Rathore SSS, Reed DE, Champagne MJ. Scale-up of a pharmaceutical roller compaction process using a joint-Y partial least squares model. *Ind Eng Chem Res*. 2011;50(18):10696–10706.
23. Reimer HL, Kleinebudde P. Hybrid modeling of roll compaction processes with the Styl'One Evolution. *Powder Technol*. 2019;341:66–74.
24. So C, Leung LY, Muliadi AR, Narang AS, Mao C. Simplifying Johanson's roller compaction model to build a "Virtual Roller Compactor" as a predictive tool - Theory and practical application. *Int J Pharm*. 2021;601:120579.
25. Sousa R, Valente PC, Nakach M, et al. Roller compaction scale-up made simple: an approximate analytical solution to johanson's rolling theory. *J Pharm Sci*. 2020;109(8):2536–2543.
26. Zinchuk AV, Mullarney MP, Hancock BC. Simulation of roller compaction using a laboratory scale compaction simulator. *Int J Pharm*. 2004;269(2):403–415.
27. Johanson JR. A rolling theory for granular solids. *J Appl Mech*. 1965;32(4):842-&.
28. Liu Y, Wassgren C. Modifications to Johanson's roll compaction model for improved relative density predictions. *Powder Technol*. 2016;297:294–302.
29. Bi M, Alvarez-Nunez F, Alvarez F. Evaluating and modifying Johanson's rolling model to improve its predictability. *J Pharm Sci*. 2014;103(7):2062–2071.
30. Moroney KM, Cronin P, Adeleye OA, et al. An evaluation of the Johanson model for roller compaction process development for a high dose API. *Powder Technol*. 2020;366:82–95.